

Large-scale upper tropospheric pollution observed by MIPAS HCN and C₂H₆ global distributions

N. Glatthor¹, T. von Clarmann¹, G. P. Stiller¹, B. Funke², M. E. Koukouli³, H. Fischer¹, U. Grabowski¹, M. Höpfner¹, S. Kellmann¹, and A. Linden¹

¹KIT – Karlsruher Institut für Technologie, Institut für Meteorologie und Klimaforschung, Karlsruhe, Germany

²Instituto de Astrofísica de Andalucía (CSIC), Granada, Spain

³Laboratory of Atmospheric Physics, Physics Department, Aristotle University of Thessaloniki, Thessaloniki, Greece

Received: 6 April 2009 – Published in Atmos. Chem. Phys. Discuss.: 29 July 2009

Revised: 3 December 2009 – Accepted: 8 December 2009 – Published: 22 December 2009

Abstract. We present global upper tropospheric HCN and C₂H₆ amounts derived from MIPAS/ENVISAT limb emission spectra. HCN and C₂H₆ are retrieved in the spectral regions 715.5–782.7 cm⁻¹ and 811.5–835.7 cm⁻¹, respectively. The datasets consist of 54 days between September 2003 and March 2004. This period covers the peak and decline of the southern hemispheric biomass burning period and some months thereafter. HCN is a nearly unambiguous tracer of biomass burning with an assumed tropospheric lifetime of several months. Indeed, the most significant feature in the MIPAS HCN dataset is an upper tropospheric plume of enhanced values caused by southern hemispheric biomass burning, which in September and October 2003 extended from tropical South America over Africa, Australia to the Southern Pacific. The spatial extent of this plume agrees well with the MOPITT CO distribution of September 2003. Further there is good agreement with the shapes and mixing ratios of the southern hemispheric HCN and C₂H₆ fields measured by the ACE experiment between September and November 2005. The MIPAS HCN plume extended from the lowermost observation height of 8 km up to about 16 km altitude, with maximum values of 500–600 pptv in October 2003. It was still clearly visible in December 2003, but had strongly decreased by March 2004, confirming the assumed tropospheric lifetime. The main sources of C₂H₆ are production and transmission of fossil fuels, followed by bio-fuel use and biomass burning. The C₂H₆ distribution also

clearly reflected the southern hemispheric biomass burning plume and its seasonal variation, with maximum amounts of 600–700 pptv. Generally there was good spatial overlap between the southern hemispheric distributions of both pollution tracers, except for the region between Peru and the mid-Pacific. Here C₂H₆ was considerably enhanced, whereas the HCN amounts were low. Backward trajectory calculations suggested that industrial pollution was responsible for the elevated C₂H₆ concentration in these particular air masses.

Except for the Asian monsoon anticyclone in September 2003, there were only comparably small regions of enhanced HCN in the Northern Hemisphere. However, C₂H₆ showed an equally strong northern hemispheric signal between the equator and low midlatitudes, persisting over the whole observation period. Backward trajectory calculations for air masses from this region also point to industrial sources of this pollution. Generally, C₂H₆/HCN ratios between 1 and 1.5 indicate biomass burning and ratios larger than 1.5 industrial pollution. However, in March 2004 ratios of up to 2 were also found in some regions of the former southern biomass burning plume.

1 Introduction

The first spectroscopic detection of atmospheric hydrogen cyanide (HCN) was reported by Coffey et al. (1981), who performed infrared absorption measurements of the total column above an aircraft. Tropospheric HCN was first discovered by ground-based spectroscopic measurements by Rinsland et al. (1982). Model calculations performed by Cicerone



Correspondence to: N. Glatthor
(norbert.glatthor@kit.edu)

and Zellner (1983), assuming HCN to be well mixed in the troposphere, slowly decreasing in mixing-ratio with altitude and lost by reaction with OH and O(¹D) in the stratosphere as well as by photolysis in the upper stratosphere, led to an estimated lifetime of 2.5 years. However, in the 1990s upper tropospheric enhancements and large seasonal variabilities were detected by ground-based FTIR measurements at several northern and southern hemispheric stations (Mahieu et al., 1995, 1997; Rinsland et al., 1999, 2000, 2001, 2002). Further, large spatial variations were found by first spaceborne measurements on the space shuttle (Rinsland et al., 1998). These observations led to the conclusion that HCN is primarily produced by biomass burning and has a tropospheric lifetime of some months only (Li et al., 2003, and references therein). Today, HCN is considered as an almost unambiguous tracer of biomass burning (Li et al., 2003; Singh et al., 2003; Yokelson et al., 2007; Crouse et al., 2009). The most significant atmospheric feature of biomass burning is a southern hemispheric plume peaking from September to November with sources in South America, Africa and Australia. Since reactions with OH and O(¹D) alone cannot compensate the biomass burning source of HCN (Rinsland et al., 2002), additional sinks like uptake by the oceans or by plants are assumed to exist (Lobert et al., 1990). Several recent papers propose ocean uptake as the main tropospheric sink of HCN. Singh et al. (2003) come to this conclusion from HCN amounts measured in the TRACE-P mission, which decrease in the mixing layer towards the ocean surface. Model calculations by Li et al. (2003), who assumed biomass burning as the only source of HCN and ocean uptake as the only sink could explain the HCN distribution measured in the TRACE-P mission and led to an estimated tropospheric lifetime of 5.3 months. The lifetime of stratospheric HCN, where the main sink is reaction with OH, is still assumed to be several years. Recent spaceborne observations of HCN are performed by the Atmospheric Chemistry Instrument (ACE) on SCISAT (Rinsland et al., 2005; Lupu et al., 2009) and by the Microwave Limb Sounder (MLS) on EOS (Pumphrey et al., 2006).

C₂H₆ is the most important non-methane hydrocarbon (NMHC) in the troposphere (Singh et al., 2001). According to Rudolph (1995) it has approximately two sources of equal importance, namely biomass burning and natural gas losses. Xiao et al. (2008) state fossil fuel production as the major source of C₂H₆, followed by biofuel and biomass burning. The tropospheric lifetime of C₂H₆ has been estimated at a few months by Rudolph and Ehhalt (1981) and at 2 months by Hough (1991). The main tropospheric loss process is reaction with OH, whereas the major stratospheric sink is reaction with Cl (Aikin et al., 1982).

In this paper we present HCN and C₂H₆ distributions derived from measurements of the Michelson Interferometer for Passive Atmospheric Sounding (MIPAS). These data represent comprehensive global datasets with ~1000 geolocations per day. The vertical coverage of the HCN dataset

extends from the upper troposphere up to 55 km, whereas the C₂H₆ profiles are restricted to the upper troposphere and lower stratosphere. Since these are the first HCN distributions retrieved from MIPAS data, we will describe the HCN retrieval method in detail, give an error estimation and present a sensitivity test. Then we will compare the global upper tropospheric HCN and C₂H₆ distributions observed between September 2003 and March 2004. This period covers the maximum and decline of the biomass burning season in South America, East and South Africa and in Australia (September to December) as well as the subsequent months with low southern hemispheric biomass burning activity. Therefore it is well suited to study the temporal evolution of the southern hemispheric biomass burning plume. Further, we will present backward trajectory calculations for air masses containing high C₂H₆ and low HCN amounts to determine the sources of the respective pollution.

2 Measurements

The Michelson Interferometer for Passive Atmospheric Sounding (MIPAS) was launched onboard the Sun-synchronous polar-orbiting European ENVIRONMENTAL SATELLITE (ENVISAT) on 1 March 2002. ENVISAT performs 14.3 orbits per day and passes the equator on its daytime downward leg at ~10:00 LT. MIPAS is a limb-viewing Fourier transform infrared (FTIR) emission spectrometer covering the mid-infrared spectral region between 685 and 2410 cm⁻¹ (4.1–14.6 μm). Its wide spectral coverage and high spectral resolution, which is 0.035 cm⁻¹ (unapodised) for the original nominal measurement mode evaluated here, enables simultaneous observation of numerous trace gases (European Space Agency (ESA), 2000; Fischer et al., 2008). This measurement mode consists of rearward limb-scans covering tangent altitudes between about 6 and 68 km within 17 altitude steps. The step-width is 3 km up to an altitude of 42 km and increases up to 8 km above 52 km altitude. MIPAS measures during day and night, covering the whole globe with about 1000 scans per day. The level-1B radiance spectra used for retrieval of HCN and C₂H₆ are data versions 4.61/4.62 (reprocessed data) provided by the European Space Agency (ESA) (Kleinert et al., 2007).

3 Retrieval method and error estimation

The HCN and C₂H₆ datasets presented in this paper were derived with the common retrieval processor of the Institut für Meteorologie und Klimaforschung and Instituto de Astrofísica de Andalucía (IMK/IAA), which was developed to produce consistent datasets containing considerably more trace species than included in the operational dataset provided under ESA responsibility. The retrievals performed with the IMK/IAA data processor consist of inversion of MIPAS level-1B spectra to vertical profiles of atmospheric state

parameters by constrained non-linear least squares fitting in a global-fit approach (von Clarmann et al., 2003). Here we refer to the HCN and C₂H₆ data versions V30_HCN_2 and V30_C2H6_11, respectively, which are the most recent ones.

Since the retrieval grid used has an altitude spacing of 1 km up to 44 km and of 2 km between 44 and 70 km, which means oversampling compared to the height distance between the tangent altitudes, application of a smoothing constraint was necessary to attenuate instabilities. Similar as for other retrievals of MIPAS data performed at IMK, Tikhonov's regularization scheme was used with a first derivative operator as constraint (Steck, 2002, and references therein). To avoid any influence of the a priori on the shape of the retrieved HCN and C₂H₆ profiles, a priori profiles with zero concentration values were chosen.

Radiative transfer calculations were performed with the Karlsruhe Optimized and Precise Radiative Algorithm (KO-PRA) (Stiller, 2000). HCN was retrieved in 10 microwindows of the ν_2 band between 715.5 and 782.725 cm⁻¹. The main differences of C₂H₆ data version V30_C2H6_11 presented here and the data version discussed in von Clarmann et al. (2007) are the use of a new set of 12 microwindows restricted to the spectral region 811.5–835.7 cm⁻¹ and the application of the HITRAN spectroscopic C₂H₆ update of 2007. Application of the new microwindows leads to considerable reduction of negative values of the C₂H₆ profiles in the UTLS region, which often occurred in the older data version. The line intensities of the new spectroscopic data, which are ~30% lower, lead to C₂H₆ volume-mixing-ratios (VMRs) enhanced by the same amount. Prior to HCN and C₂H₆ several other quantities are inferred in the retrieval chain. First, spectral shift, the temperature profile and the tangent heights are fitted, followed by retrieval of the abundances of H₂O, O₃, CH₄, N₂O, HNO₃, ClONO₂, ClO, N₂O₅, CFC-11, CFC-12, NO₂, and HNO₄. The fitted profiles of all these species are used to model their radiative contributions, if they are interfering species in the HCN and C₂H₆ microwindows. Further, the fitted C₂H₆ profiles are used for HCN retrievals. The following additionally interfering species are accounted for in the radiative transfer modelling on the basis of climatological profiles (Kiefer et al., 2002; Remedios et al., 2007): CO₂, NH₃, OCS, C₂H₂, COF₂, C₂H₄, CFC-22, CFC-113 and PAN for both targets; additionally CH₃Cl, CH₃CCl₃, CCl₄, HCFC-141a, and acetone for HCN retrievals as well as HCN and CFC-114 for C₂H₆ retrievals. Except for CO₂ the radiative contribution of these additionally interfering species is rather small and thus modelling of their radiance contribution by climatological rather than by pre- or joint-fitted profiles is justified. Further, the volume mixing ratio of CO₂ is well known and its spectral signature had implicitly been fitted in the preceding temperature retrieval. Along with the HCN and C₂H₆ profiles, microwindow-dependent continuum radiation profiles and microwindow-dependent, but height-independent zero-level calibration corrections are jointly fitted.

Figure 1 characterises a HCN profile obtained on 21 October 2003 inside the biomass burning plume over East Africa (12.9° S, 37.2° E). For similar information on C₂H₆ we refer to von Clarmann et al. (2007). The HCN volume-mixing-ratio (top left) reveals enhanced values in the troposphere, namely 470 pptv at the lowermost cloud-free height (11 km) and 350 pptv at the tropopause (17 km), and background values between 200 pptv in the lower and 100 pptv in the upper stratosphere. The respective vertical resolution is better than 4 km up to 14 km altitude, but degrades to 10 km around the cold tropopause (17 km) (top right). In the in turn warmer lower and middle stratosphere the height resolution is better again, namely 6–7 km. In the upper stratosphere it degrades to 10 km because of the coarser vertical tangent spacing. The total estimated HCN precision, including instrumental noise and random parameter uncertainties, for this geolocation is between 10 and 15% in the troposphere and increases to 50% at 55 km altitude (bottom left). The estimated standard deviation (error bars top left and dotted line bottom left) increases from 6% at 11 km to 50% at 55 km altitude. The dominating error components are uncertainties in the pointing of the instrumental line of sight (in terms of elevation) in the upper troposphere, uncertainties in spectral shift in the lower stratosphere and measurement noise (estimated standard deviation) in the middle and upper stratosphere. Except for O₃ and CO₂ the error contribution of interfering species is less than 1% and therefore not shown. This error estimate is based on the actual retrieved temperatures, tangent heights, HCN profiles and simulated spectra and Jacobians of the final iteration. Details of the error estimation scheme are reported in, e.g., Glatthor et al. (2004). To estimate the total HCN accuracy, systematic errors have also be taken into account. The major systematic error source not shown in Fig. 1 (bottom left) is the spectroscopic uncertainty of 5–10% both for HCN line intensities as well as for the air broadened half-width (Rothman et al., 2005), translating into a similar systematic HCN uncertainty. Figure 1 (bottom right) shows the HCN signature at 13.0 km altitude at the East African geolocation, expressed as difference between the model spectrum containing the retrieved HCN amount (460 pptv) and a model spectrum for the same, but HCN-free atmosphere. According to this estimation there are ~12 HCN lines with signal-to-noise ratios between 2 and more than 10 in this spectral region.

To verify the robustness of the HCN results, we also performed retrievals without consideration of HCN as fit parameter as well as in atmospheric modelling. The only variable parameters in this case were continuum and offset. The result of this approach for the East African geolocation is shown in Fig. 2, which contains measured and modelled spectra in the region of the HCN microwindows for tangent altitudes of 13.0 km (top left) and 30.4 km (top right). The residuals (bottom row) without consideration of HCN (red) increased significantly compared to those from the HCN fit (blue), namely from 33.7 to 64.6 nW/(cm² sr cm⁻¹) at 13 km (left) and from

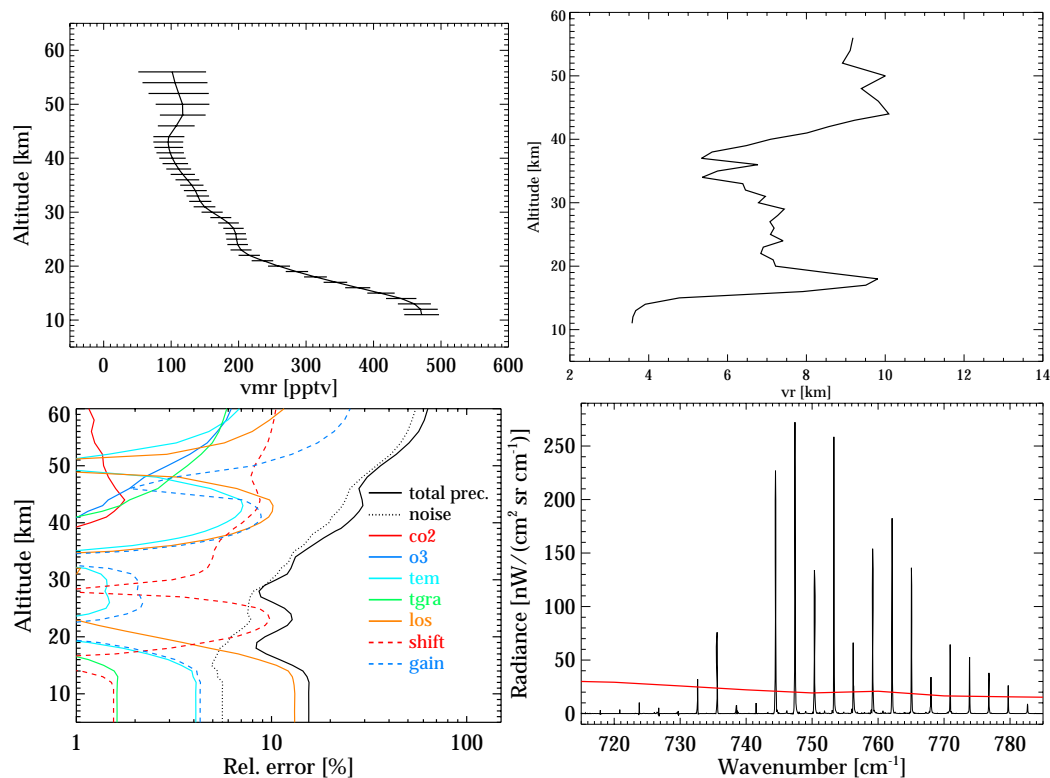


Fig. 1. Top left: HCN vmr-profile measured by MIPAS on 21 October 2003, inside the biomass burning plume over East Africa (12.9° S, 37.2° E); the error bars represent measurement noise. Top right: Height resolution for the same geolocation. Bottom left: Total HCN precision (solid line), noise error (dotted line) and contributions of major random parameter errors (uncertain knowledge on CO₂ (co2) and O₃ mixing ratio (o3), temperature (tem) and temperature gradients (tgra), pointing of the instrumental line of sight (los), spectral shift (shift) and calibration (gain) of the measured spectra). Bottom right: HCN spectral signature at the same geolocation at 13 km altitude, expressed as difference between the model spectrum of the HCN fit and a spectrum calculated for the same, but HCN-free atmosphere. The red curve displays the instrumental NESR.

17.8 to 20.4 nW/(cm² sr cm⁻¹) at 30.4 km (right), i.e. by 92% and 15% respectively. This result confirms that a sufficient number of HCN lines is not masked by signatures of other constituents. Figure 3 exemplarily exhibits a zoom of the left panel of Fig. 2 for the spectral region around the microwindow 744.35–744.5 cm⁻¹ (black line) along with the radiance contribution of several prefitted trace gases and of fitted HCN. The main contribution to the spectral radiance in the whole region results from CO₂, O₃ and HCN (left panel). The additional zoom in radiance (right panel) illustrates the contributions of N₂O₅ and H₂O and that in the microwindow itself HCN accounts for the second largest radiance contribution. The residual in the region of the microwindow (bottom row) is below ±50 nW/(cm² sr cm⁻¹) and in the extended region below ±90 nW/(cm² sr cm⁻¹). This shows that even in the region not used for analysis the measured spectrum is reasonably well modelled using the prefitted trace gases.

4 Upper tropospheric HCN and C₂H₆ from September 2003 to March 2004

The analysed dataset consists of 54 days of the period 8 September 2003 to 25 March 2004. This period contains the maximum (September–October) and end (December) of the 2003 southern hemispheric biomass burning season (cf. Edwards et al., 2006) and the subsequent months January to March 2004 with nearly no southern hemispheric burning activity. Our data sampling is good from September to November (10–20 evaluated days per month) but becomes sparse thereafter, where only 3–5 days per month have been analysed so far.

4.1 HCN and C₂H₆ on 21 October 2003

To demonstrate the capabilities of single-scan data (not averaged), Figure 4 shows the global HCN (left) and C₂H₆ (right) distributions retrieved for a single day, 21 October 2003, at 12 km altitude. These daily distributions contain large data gaps (white areas), mainly located in the tropics and

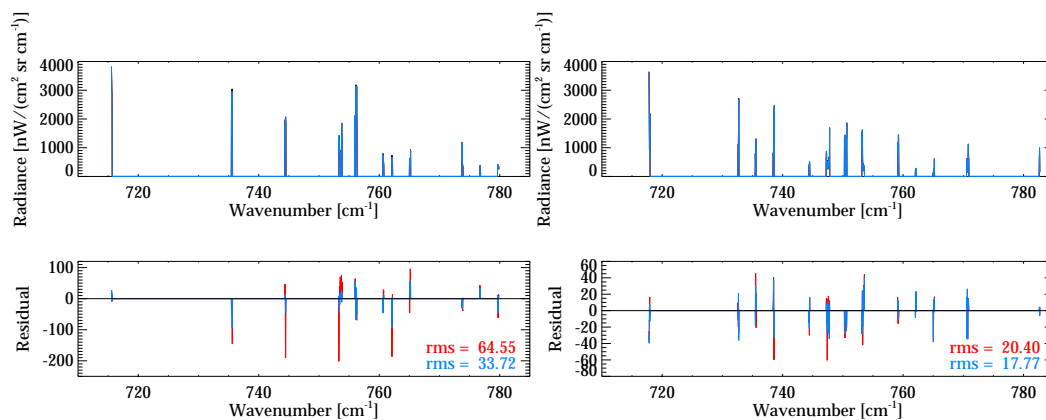


Fig. 2. Measured and best-fit spectra (upper panel) and residuals (lower panel) for MIPAS measurements obtained on 21 October 2003 over Eastern Africa (12.9° S, 37.2° E) on 13.0 km (left) and 30.4 km altitude (right). Measured spectra (black) are largely covered by the model spectra. Blue spectra and residuals represent results from our standard retrieval with fit variables $\text{vmr}(\text{HCN})$, continuum and offset. Red residuals refer to a fit, where $\text{vmr}(\text{HCN})$ was fixed at zero mixing ratio. Only radiances in HCN microwindows plotted.

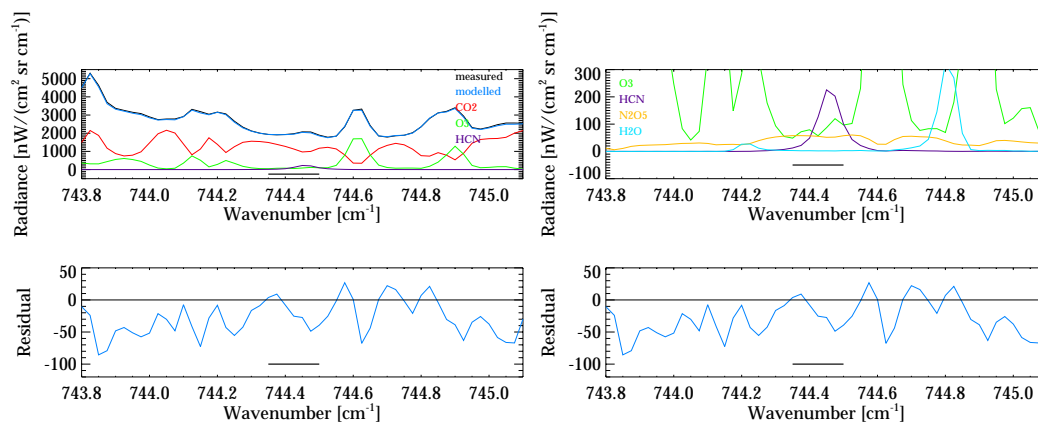


Fig. 3. Left: Zoom of left panel of Fig. 2 for the spectral region around the microwindow $744.35\text{--}744.5\text{ cm}^{-1}$ (denoted by black line) with measured spectrum (black), modelled spectrum of the HCN retrieval (blue) and radiance contribution of CO₂ (red), O₃ (green) and HCN (violet). The bottom panel contains the residual (blue). Right: Same as left, but additional zoom of the radiance axis to emphasise the contributions of HCN (violet) N₂O₅ (brown) and H₂O (light blue).

subtropics, which are caused by rejection of tropospheric measurements due to cloud contamination. However, in good agreement both HCN and C₂H₆ already show one of the main features of our dataset, namely the central part of the southern hemispheric biomass burning plume as contiguous area of high VMRs extending from the Southern Atlantic to East Africa. Interrupted by data gaps, this area extends eastward above the Southern Indian Ocean as far as Australia and the South Pacific. Furthermore there are more or less uniform HCN amounts between northern subtropics and high latitudes, indicating similar HCN values in the upper troposphere and lower stratosphere. On the contrary the northern C₂H₆ distribution exhibits high values in the tropics and subtropics but considerably lower amounts in mid and high latitudes, which hints at tropospheric industrial pollution and

stronger decrease above the tropopause. All these features will be discussed more in detail in the next subsection. Further there is some indication for regional variations, e.g. enhanced HCN amounts above Central Asia and Northern India. However, these patterns exhibit only low statistical significance.

4.2 Temporal development of HCN and C₂H₆

In the following discussion we use monthly means to enhance the spatial data coverage and to decrease statistical uncertainties. Figure 5 shows zonal averages of HCN and C₂H₆ of October 2003 and March 2004, i.e. from the peak of the southern hemispheric biomass burning season and from some months thereafter. The latitudinal binning consists of 5°-bands containing typically 20–170 datapoints at upper

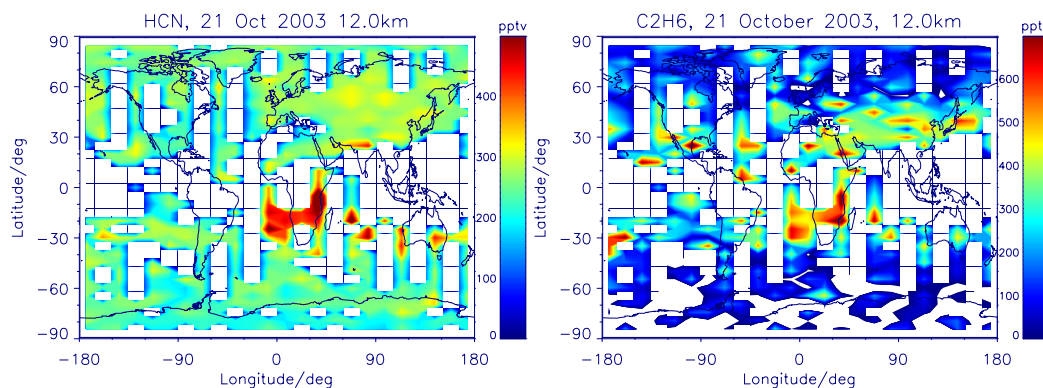


Fig. 4. Global HCN (left) and C₂H₆ (right) distributions on 21 October 2003 at 12 km altitude, obtained from MIPAS data. The white areas are bins containing no measurements and data gaps due to cloud contamination or, in case of C₂H₆, insensitive data south of 60° S.

tropospheric height levels. In October, MIPAS observed a distinct plume of enhanced HCN amounts (top left) of up to 350 pptv in the tropical to midlatitude Southern Hemisphere, covering the altitude region 8 to 16 km. On the contrary the northern hemispheric tropics and midlatitudes exhibited background HCN amounts (~240 pptv) only. Probably due to boreal fires HCN at northern high latitudes was moderately enhanced to ~270 pptv. In March 2004 the southern hemispheric plume of enhanced HCN had disappeared (bottom left). Moreover, this region now exhibited the lowest tropospheric HCN values, whereas the northern midlatitude HCN mixing ratios below 10 km were slightly enhanced in comparison to the other latitude bands. Unlike HCN, the C₂H₆ distribution of October 2003 (top right) was more symmetric around the equator. Apart from a southern hemispheric plume of up to 400 pptv of similar extent as observed in HCN (cf. von Clarmann et al., 2007), C₂H₆ exhibited a comparably large region of even somewhat higher values between the northern hemispheric tropics and midlatitudes. Further, C₂H₆ showed a much stronger decrease towards the stratosphere than HCN. In March 2004 the southern hemispheric feature of enhanced C₂H₆ was considerably reduced, whereas the northern hemispheric C₂H₆ plume was restricted to lower latitudes, but contained just as high amounts as in October.

Figures 6 and 7 show HCN and C₂H₆ distributions of September, October, December 2003 and of March 2004 on pressure levels of 200 hPa (10.5–12.6 km) and of 125 hPa (13.5–15.5 km). The latitude-longitude binning applied here and in Fig. 9 is 5° × 15°, with typically 5–15 datapoints per bin. As already mentioned above, both pollutants exhibited enhanced values in the southern hemispheric biomass burning plume region, with VMRs of up to 500–600 pptv from September to December 2003. The HCN plume was most pronounced in October and slightly weaker in September and December. It extended nearly globally from the east coast of Tropical South America over Central and South

Africa and Australia to the subtropical and midlatitude Southern Pacific. The potential to produce the shape of this plume by biomass burning was shown by trajectory calculations starting above clusters of fire counts in South America, Africa and Australia by von Clarmann et al. (2007). Further, a similar plume was found in the same time period in the PAN distribution obtained from MIPAS data (Glatthor et al., 2007). In March 2004 the HCN plume had nearly disappeared, which reflects the seasonal variation of southern hemispheric biomass burning and confirms the proposed lifetime of tropospheric HCN of some months (Li et al., 2003). The southern hemispheric biomass burning plume of enhanced HCN generally also revealed elevated C₂H₆ amounts peaking in September and October 2003. Like for HCN, there was still a clear C₂H₆ signal in December, followed by a strong decrease in March 2004. The C₂H₆ decrease was, however, somewhat less pronounced than that of HCN. Strikingly, in September and October 2003 enhanced southern hemispheric C₂H₆ amounts were also measured between Peru and the tropical mid-Pacific, whereas the HCN values in this region were low. The source region of these polluted air masses will be determined by backward trajectory calculations in Sect. 5.1.

In the Northern Hemisphere, HCN enhancements on the 200 hPa pressure level were less pronounced and covered considerably smaller areas, mainly the tropical Atlantic in September and a region extending from Northeast Africa to the Middle East in October 2003. The same applies for northern hemispheric HCN on 125 hPa except for September, when a large area of enhanced HCN was observed between the Middle East and Southern China (Fig. 7, top left). As outlined in Funke et al. (2009) and Park et al. (2008), this feature, which is even more pronounced in C₂H₆ (Fig. 7, top right), is due to trapping of polluted air masses in the Asian monsoon anticyclone (AMA). Although our dataset also covers the northern tropical biomass burning season (February to May), there was also no strong northern hemispheric HCN

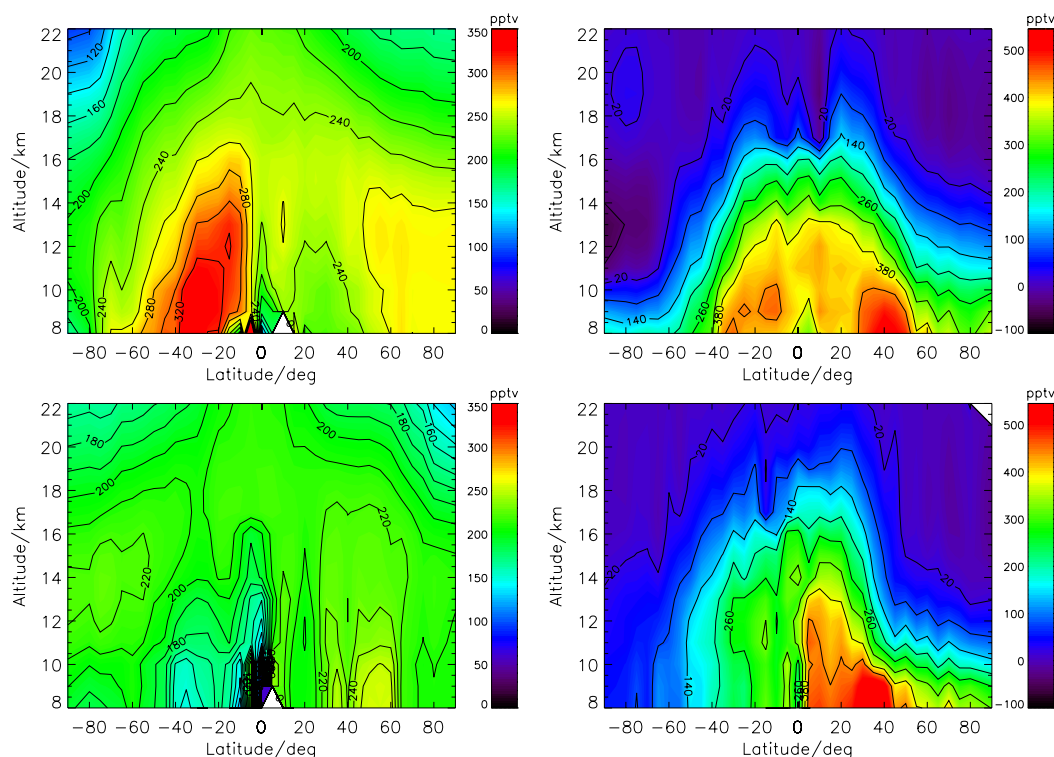


Fig. 5. Top: Zonally averaged HCN (left) and C₂H₆ (right) distributions of October 2003. Bottom: Zonally averaged HCN (left) and C₂H₆ (right) distributions of March 2004.

enhancement in March 2004, maybe due to less biomass burning during this season. In contrast to HCN, C₂H₆ showed just as high values in the whole northern hemispheric tropics and subtropics as in the Southern Hemisphere with several “hot spots”: One above the Atlantic during the whole observation period and another one extending in September from North-East Africa to South Asia. Furthermore, there was a region of enhanced values reaching from China and Japan to the West Coast of North and Central America with peak values in December and another spot above the Caribbean Sea and the Gulf of Mexico. All these C₂H₆ enhancements not accompanied by high HCN are suspected to be caused by industrial or urban activities and not by biomass burning, because the latter would go along with HCN enhancements. This question will be investigated more closely in the following section by backward trajectory calculations.

Air masses at the 200 hPa level generally belong to the troposphere from the tropics to low midlatitudes and to the stratosphere at higher latitudes, whereas at 125 hPa the transition is shifted equatorward to the subtropics. For both altitudes we calculated the monthly mean tropopause intersection (red lines in Figs. 6 and 7) from the National Centers for Environmental Prediction (NCEP) reanalysis data (<http://www.cdc.noaa.gov/data/gridded/data.ncep.reanalysis.html>). The C₂H₆ distribution generally shows a sharp poleward decrease at the NCEP tropopause

intersection, which confirms the capability to differentiate between tropospheric and stratospheric air masses from the C₂H₆ retrieval. Some areas of moderately enhanced C₂H₆ values poleward of the northern intersection might indicate smearing from tropospheric pollution below due to limited height resolution of the MIPAS retrievals, but can also well be caused by short-term (duration of some days) northward excursions of the intersection associated with northward transport of polluted air masses. E.g. Funke et al. (2009) showed that high CO on 21 October 2003 over the North Atlantic and Greenland was caused by a northward stream of midlatitude air masses at this time. This feature is also visible, though attenuated due to averaging over a whole month, in the October C₂H₆ data presented here. On the contrary, the HCN distribution exhibits only moderate gradients at the tropopause intersection, except for the southern hemispheric plume and for the AMA region. This reflects the more gradual transition from tropospheric to stratospheric HCN due to its longer stratospheric lifetime.

Figure 8 depicts monthly mean profiles of HCN in and above the central region of the southern hemispheric biomass burning plume (0°–40° S, 60° W–120° E), normalized by the October values. The HCN amounts of September and November 2003 are above 90% of the October-values in the whole troposphere, and even in December 2003 still above 80%. This reflects a persistent biomass burning plume from

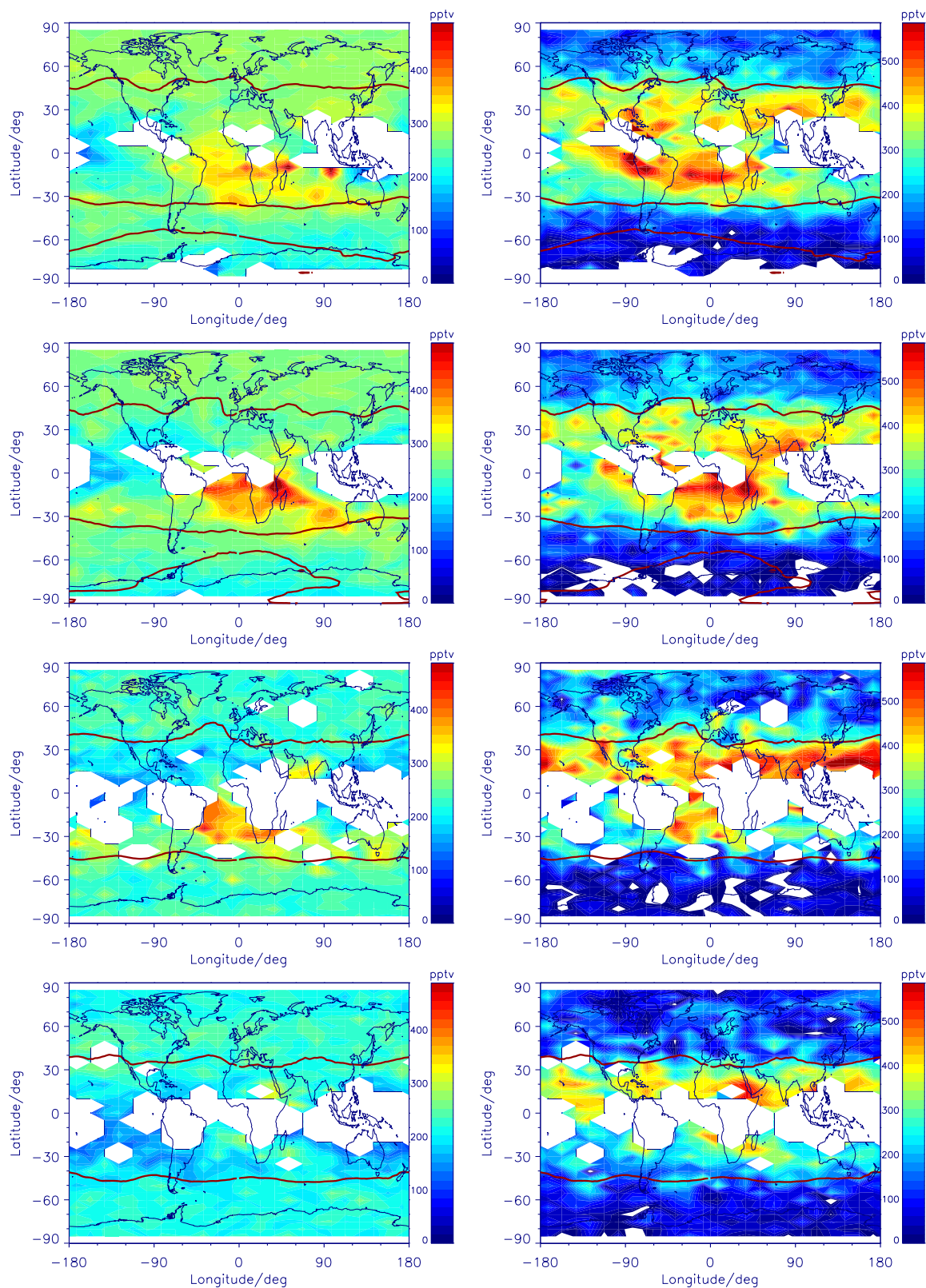


Fig. 6. Left: Global HCN distribution at 200 hPa (10.5–12.6 km) in September, October, December 2003 and in March 2004 (top to bottom). Right: Same as left but for C₂H₆. The white areas are data gaps due to cloud contamination (or insensitive values in case of C₂H₆ south of 60° S). Red solid lines show the tropopause intersection from the NCEP reanalysis.

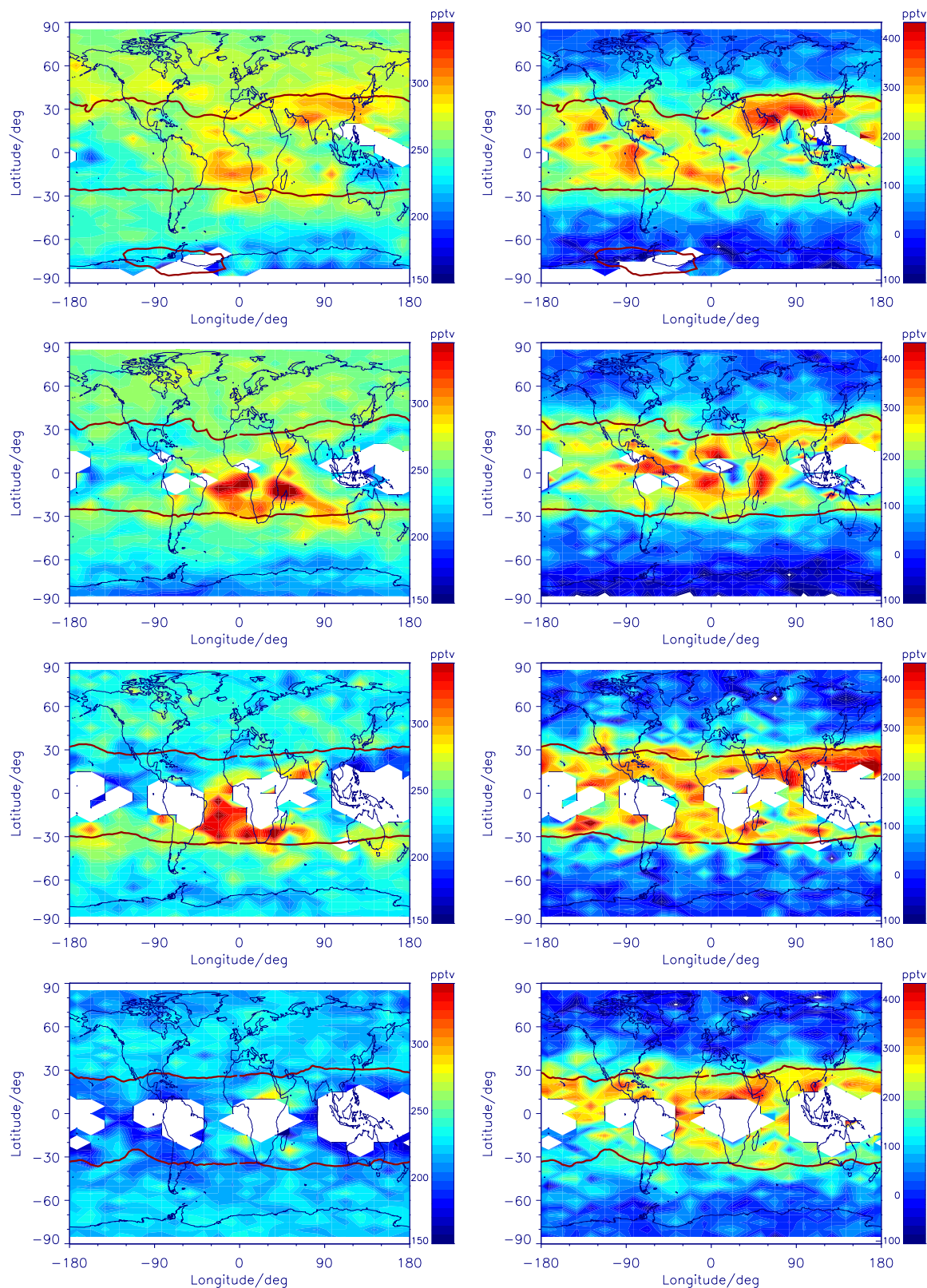


Fig. 7. Left: Global HCN distribution at 125 hPa (13.5–15.5 km) in September, October, December 2003 and in March 2004 (top to bottom). Right: Same as left but for C₂H₆. The white areas are data gaps due to cloud contamination. Red solid lines show the tropopause intersection from the NCEP reanalysis.

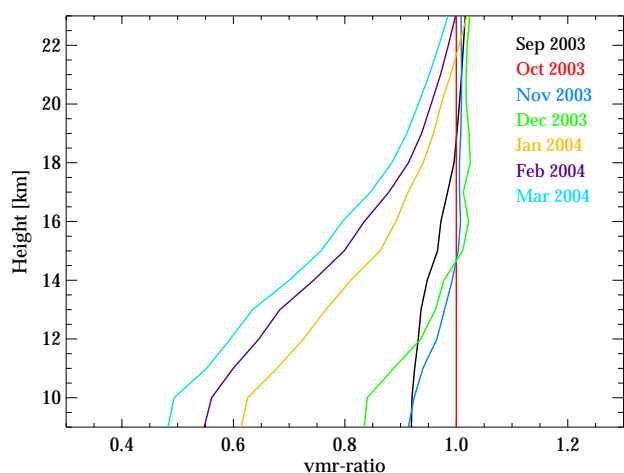


Fig. 8. Monthly averaged HCN profiles measured above the central southern hemispheric biomass burning region (0°–40° S, 60° W–120° E) for the time period September 2003 to March 2004, normalized by the October profile.

September to December. However, the ratios of the following months are considerably reduced, namely at 9 km altitude to 62% in January, to 55% in February and to 47% in March 2004. Towards higher altitudes the reduction becomes lower, e.g. the January–March ratios at 14 km are 82, 74 and 69%. These data allow a simple estimation of the lifetime of HCN under the assumption that the biomass burning activities ended at the end of October and that HCN decreased exponentially thereafter. The end of biomass burning at the end of October was estimated based on Fig. 5 in Edwards et al. (2006), which shows a sharp decrease in tropical and southern hemispheric MODIS fire counts after October 2003. For the altitude of 9 km this approximation resulted in an e-folding lifetime of 6.2–6.9 months for HCN measured in January to March 2004, which is in reasonable good agreement with the most recent estimate of the tropospheric lifetime of 5.3 months of Li et al. (2003). The difference could be due to the fact that the estimate of Li et al. (2003) is an average of the whole troposphere, whereas our estimate was derived for the upper troposphere, from where downward transport and ocean uptake of HCN might last longer. The same reason might at least partly apply for the considerably longer HCN lifetime calculated from MIPAS data for the altitude of 14 km, namely 13.5–14.3 months.

4.3 Regional differences between the C₂H₆ and HCN distributions

Since C₂H₆ is an indicator of industrial pollution as well as of biomass burning, whereas HCN is a rather unambiguous indicator of the latter process only, the chemical composition of plume air should be useable to assign air parcels to either biomass burning or industrial pollution

(“chemical fingerprint method”). To highlight the differences between the C₂H₆ and HCN distributions, Fig. 9 shows the C₂H₆/HCN ratio at 200 hPa between September 2003 and March 2004. In September, October and December 2003 the ratios in the southern hemispheric biomass burning region, extending from the east coast of tropical South America over Africa and Australia to the midlatitude Southern Pacific, are mostly between 1 and 1.5. In March 2004 they reach values of up to 2, probably due to a stronger reduction of HCN and industrial pollution from Indonesia and Malaysia. Another reason might be open cooking fires, which are common all year round in the region of former Southern African biomass burning and also produce high C₂H₆/HCN ratios (Bertschi et al., 2003). During September and October the highest ratios of up to 2 are found in a large area between the tropical central Pacific and northern South America (“Galapagos region”), further above the northern tropical East-Pacific, the Caribbean Sea, the Gulf of Mexico and the adjacent Atlantic. Apart from the Galapagos region, the ratios in the northern hemispheric tropics and subtropics are generally higher than in their southern hemispheric counterparts. In December 2003 the ratios in this region form a nearly contiguous band of values of even up to 3 due to very high C₂H₆ but low HCN amounts. In March this band has become somewhat weaker, but still exhibits ratios of up to 2. In summary, Fig. 9 indicates a threshold ratio of ~1.5 to distinguish between biomass burning and industrial pollution. In Sect. 5 we will investigate several representative regions with high C₂H₆/HCN ratios (black rectangles in Fig. 9) in more detail, using backward trajectory calculations in order to identify possible industrial sources favoring elevated C₂H₆ and to investigate if this “chemical fingerprint method” is robust and can be applied to MIPAS data.

4.4 Comparison with other space-, airborne and ground-based measurements

Unfortunately, independent global HCN or C₂H₆ data are not available for the time of our analysis. However, the extent of the biomass burning plume detected in the MIPAS HCN and C₂H₆ distributions is in good agreement with the area of enhanced CO measured during the last week of September 2003 by the Measurement of Pollution in the Troposphere (MOPITT) instrument on the Terra satellite (Edwards et al., 2006), which is also attributed to biomass burning. On the 250 hPa pressure level (~10 km) the CO plume extended from tropical Brasil over the Southern tropical and subtropical Atlantic, Southern Africa to the Indian Ocean. In terms of MOPITT CO column amounts the plume extended even further over Australia and the Pacific Ocean. The consistency between the MIPAS HCN and MOPITT CO mixing ratios of September 2003 was verified by calculation of their enhancement ratio and comparison with values given in the literature. On the 250 hPa level the $\Delta\text{HCN}/\Delta\text{CO}$ enhancement ratio, estimated from values in the central part

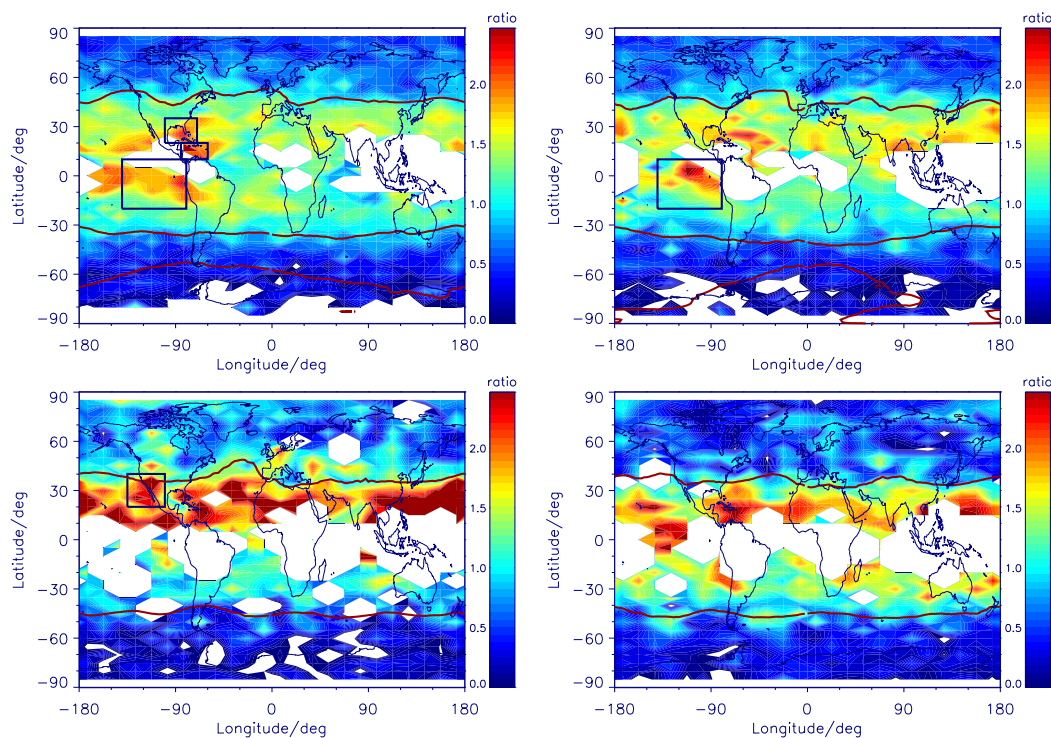


Fig. 9. Global C₂H₆/HCN ratio at 200 hPa in September, October, December 2003 and in March 2004 (top left to bottom right). The white areas in the tropics and subtropics are data gaps due to cloud contamination (white areas at high southern latitudes are negative values). Blue rectangles indicate regions, for which HYSPLIT backward trajectory calculations were performed (see Figs. 10–12).

and in remote parts of the plume is ~ 0.0028 . This value is in good agreement with the average $\Delta\text{HCN}/\Delta\text{CO}$ enhancement ratio of 0.00341 ± 0.00153 given by Singh et al. (2003) for biomass burning plumes in the upper troposphere (3–12 km) above the Pacific Ocean. HCN/CO emission ratios, measured in direct proximity of savanna fires in Southern Africa are somewhat higher, namely 0.0085 ± 0.0029 (Yokelson et al., 2003). There is also qualitatively good agreement of the biomass burning plume obtained from MIPAS data with the HCN and C₂H₆ distributions measured between September and November 2005 by the Fourier Transform Spectrometer (FTS) on the ACE/SCISAT-1 satellite (Coheur et al., 2007). Both the “HCN-plumes” and “C₂H₆-plumes” agree fairly well in location and in magnitude of the mixing-ratios. A more detailed comparison can be made with the ACE HCN data in Lupu et al. (2009). These authors present monthly mean HCN data of six latitude bands, measured by ACE between February 2004 and January 2007. At 8.5 km altitude the ACE HCN values for the latitude band 0–30° S, which contains the major part of the southern biomass burning plume, are about 430, 450 and 470 pptv in October 2004, 2005 and 2006, respectively. The according values at 13.5 km altitude are around 370, 370 and 475 pptv. The MIPAS HCN data of October 2003 are somewhat lower in this latitude band, namely up to 330 pptv at 8.5 km and up to 300 pptv at 13.5 km altitude (cf. Fig. 5, top left). Restricted

to the longitudinal extent of the biomass burning plume of October 2003, the MIPAS HCN amounts are 380 pptv at 9 km altitude, which is closer to the ACE data. For background conditions there is good agreement between the HCN amounts measured by ACE and MIPAS. E.g. the ACE values of the latitude band 0–30° S are around 180 pptv in February 2005 and 2006 at 8.5 and 13.5 km, which is nearly identical to the HCN amounts measured by MIPAS in March 2003 in this altitude region (cf. Fig. 5, bottom left).

The northern tropical to midlatitude HCN data of MIPAS are in good agreement with in-situ data obtained during the NASA TRACE-P airborne mission from February to April 2001 (Singh et al., 2003; Li et al., 2003). These authors report mean values of 260 pptv at 9 km and 240 pptv at 11 km altitude over the Northern Pacific (10° N–40° N), whereas the respective MIPAS values are 220–240 pptv (Fig. 5).

There is also qualitatively good agreement with ground-based FTIR measurements from Wollongong (34° S) in Australia (Rinsland et al., 2001). Between July 1997 and February 1998 this instrument measured nearly height-independent HCN values around 200 pptv in the altitude region 3 to 20 km during background conditions. For the biomass burning period (August–December 1997) the mean HCN amounts increased from 300 pptv at 5 km to 400–430 pptv at 11 km. Above they decreased linearly to 180–200 pptv at 20 km altitude. In comparison, the southern

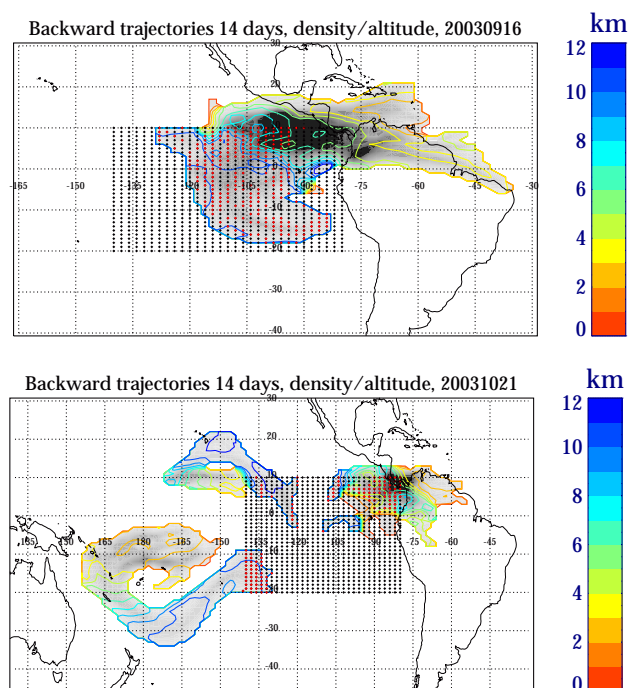


Fig. 10. Top: 14-day backward trajectories calculated with the HYSPLIT model, ending on 16 September 2003 at 10 km altitude over the Pacific region west of northern South America. Backward trajectories have been calculated for the area covered with red and black points, but only those originating at altitudes below 3.5 km have been considered. End points of rejected and considered trajectories are indicated by black and red points, respectively. Colour contours and grey-shading show mean trajectory altitude and density. Bottom: Same as top, but for 21 October 2003.

midlatitude HCN values measured by MIPAS in the altitude region 10–20 km were between 170 and 210 pptv for background conditions (Fig. 5, bottom left) and around 320 pptv at 10 km in the biomass burning plume (Fig. 5, top left).

5 Backward trajectory calculations

5.1 Galapagos region in September and October 2003

During the biomass burning period the region extending from the mid-Pacific to South America (“Galapagos region”) is the only area in the Southern Hemisphere with high C₂H₆ but low HCN (Figs. 6, 7 and 9). This feature is especially pronounced in September and October 2003. Von Clarmann et al. (2007) attribute southern hemispheric C₂H₆ enhancements predominantly to biomass burning, but the simultaneously measured low HCN amounts in this region suggest another source of pollution. To clarify the origin of these air masses, 14-day backward trajectory calculations (which is still short compared to the C₂H₆ lifetime of 60 days or more, cf. Sect. 1) were performed for 16 September

and 21 October 2003 with the HYbrid Single-Particle Lagrangian Integrated Trajectory (HYSPLIT) model (Draxler and Hess, 1998), basing on meteorological data from the National Centers for Environmental Prediction (NCEP) reanalysis (Kalnay et al., 1996). In doing so a similar statistical analysis for numerous (961) trajectory endpoints covering the Galapagos region at 10 km altitude as described in Funke et al. (2009) was performed, by which random errors of single trajectory locations cancel out (Draxler, 1991). Accordingly, only trajectories originating at altitudes below 3.5 km, i.e. enabling transport of potentially polluted air masses from the boundary layer into the free troposphere, were taken into account for analysis (red ending points in Figs. 10–12), whereas all other trajectories were neglected (black ending points). The calculations for 16 September (Fig. 10, top) show that the air masses with high C₂H₆ in the Galapagos region (cf. Figs. 6 and 9) were lofted into the free troposphere mainly above the northern part of South America and the Caribbean Sea, where the backward trajectories were at altitudes of 3.5 km or below (orange and yellow curves). On 21 October the investigated area is only sparsely covered with ending points of HYSPLIT backward trajectories, which had travelled through the boundary layer during the preceding 14 days (Fig. 10, bottom). The air masses in the northeastern part of the analyzed area obviously also entered the free troposphere above northern South America. Unfortunately the major part of these ending points is in a region with no MIPAS data due to cloud coverage. However there is at least a small overlap with the region of high C₂H₆/HCN ratios southwest of this data gap (cf. Fig. 9, top right), indicating the same source region for these polluted air masses. On the contrary, the air masses with low C₂H₆/HCN ratios in the northwestern and southwestern part came from the remote tropical Pacific. According to fire counts of the Tropical Rainfall Measuring Mission (TRMM) satellite (Giglio, 2000), there was no burning activity in northern South America during September and only very limited activity in October. Therefore we conclude that the enhanced C₂H₆ amounts were caused by the considerable oil and gas production in Venezuela and Trinidad and Tobago (<http://www.cia.gov/library/publications/the-world-factbook>) or other industrial pollution in this region. On the other hand, the low C₂H₆/HCN ratios of the northwestern and southwestern air masses are in good agreement with their marine origin.

5.2 Caribbean Sea and Gulf of Mexico

Other regions of enhanced C₂H₆ but background HCN are the Caribbean Sea and the Gulf of Mexico (Figs. 6, 7 and 9). To determine the origin of these polluted air masses HYSPLIT calculations were performed for 16 September 2003, and ending points covering these regions at 12 (Caribbean Sea) and 10 km altitude (Gulf of Mexico), whereby in this case 20-day backward trajectories were necessary to obtain a reasonably clear classification. These calculations suggest

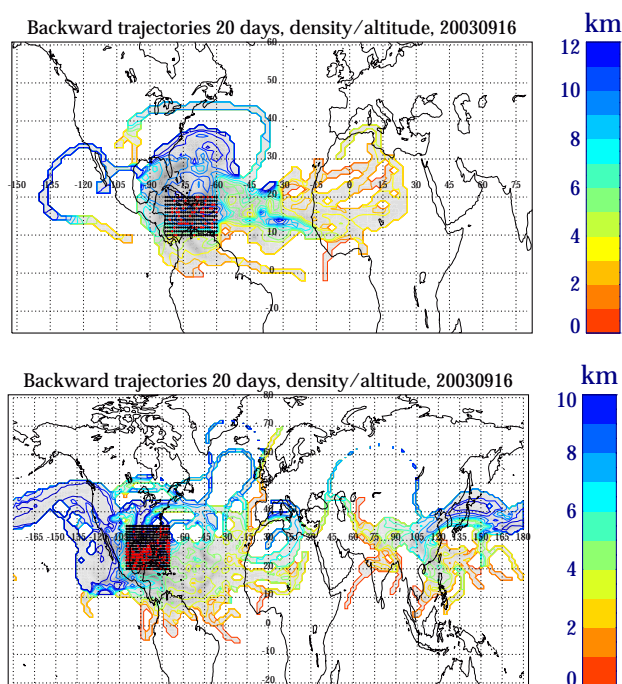


Fig. 11. 20-day backward trajectories calculated with the HYSPLIT model, ending on 16 September 2003 at 12 km altitude over the Caribbean Sea (top) and at 10 km altitude over the Gulf of Mexico (bottom). For more details see Fig. 10.

that one portion of the air masses above the Caribbean Sea (Fig. 11, top) originated in northern South America, where, as outlined above, no biomass burning activity occurred during this time of the year. The other fraction came from the Sahara desert and Sahel region in northern Africa. According to TRMM fire counts there was also no biomass burning in the Sahel zone in September 2003. Therefore we conclude that the enhanced Caribbean C₂H₆ values also resulted from the oil or gas industry or other industrial activities in northern South America or in Northern Africa. The main pollution sources of the air masses above the Gulf of Mexico (Fig. 11, bottom) were obviously also in northern South America and to a certain extent in South Asia, where biomass burning activity was low, too. Thus, the backward trajectories ending above the Gulf of Mexico also point to oil or gas production or industrial pollution as source of the high C₂H₆ amounts measured there.

5.3 South Asian monsoon region in September 2003

As stated above, especially in September 2003 the region extending from the Arabian Peninsula over India to southern China displays another “hot spot” of enhanced C₂H₆ both at 200 and at 125 hPa. To a somewhat lesser extent, this feature is also visible in HCN on the latter pressure level. As outlined in Funke et al. (2009), the high amounts of CO measured by MIPAS in this area reflect trapping of polluted air masses

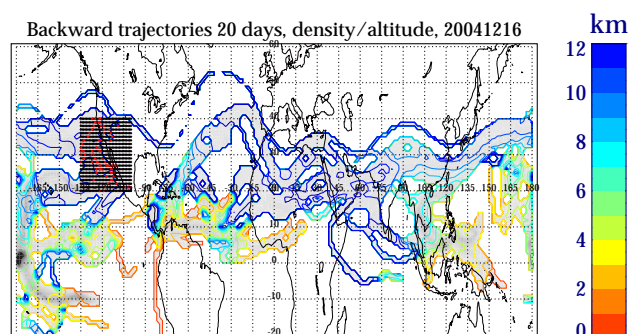


Fig. 12. 20-day backward trajectories calculated with the HYSPLIT model, ending on 16 December 2003 at 12 km altitude over the North American West Coast. For more details see Fig. 10.

in the Asian monsoon anticyclone. By a statistical analysis using HYSPLIT trajectories for 10 September 2003, these authors have shown that the pollutants in the monsoon anticyclone were injected into the free troposphere mainly over Bangladesh and Southeast China, where biomass burning was low at the beginning of September. Thus they assumed industrial and urban emissions as the most likely source, which explains the high C₂H₆ amounts presented here. However, they also found indication for a smaller contribution from Indonesian biomass burning, which is confirmed by our finding of elevated HCN values. For comparison, Park et al. (2008) also found high HCN amounts in the Asian monsoon anticyclone during June to August 2004–2006.

5.4 Trans-Pacific transport in December 2003

A fourth region of enhanced C₂H₆ but background HCN is the Pacific Ocean between China/Japan and the North- and Central-American West Coast. This feature is more or less persistent over the whole observation period, but especially pronounced in December 2003. 20-day HYSPLIT backward trajectory calculations for 16 December 2003, and several hundred ending points at 12 km altitude above the North American West Coast (Fig. 12) indicate mainly three injection regions of these air masses into the free troposphere, namely the southern hemispheric Pacific, Northern South America and Indonesia/Malaysia. The Southern Pacific is largely out of question for the pollution in the investigated region, because this region contains no industrial sources. Thus northern South America and Indonesia remain as possible sources. According to TRMM fire counts there was nearly no biomass burning in both regions during December. However, as already outlined above, there is considerable oil and gas production in northern South America and even more in Indonesia and Malaysia (<http://www.cia.gov/library/publications/the-world-factbook/fields>), which we consider as source of the high C₂H₆. For comparison, Funke et al. (2009) have identified somewhat more northern Asian regions, namely Northern India and Southern China, as sources

of pollution in front of the West Coast of the United States on 10 September 2003.

6 Summary and conclusions

We have compared global upper tropospheric HCN and C₂H₆ distributions derived from MIPAS/ENVISAT data. HCN was retrieved from MIPAS spectra for the first time, whereas the C₂H₆ retrieval has already been presented in von Clarmann et al. (2007). The HCN analysis was performed in 10 microwindows in the spectral region 715.5–782.7 cm⁻¹. Significant HCN profiles were obtained between 8 and 55 km, with a height resolution decreasing from 5 to 11 km with increasing altitude. The total estimated precision is 10–15% for enhanced upper tropospheric HCN inside the biomass burning plume and about 50% for HCN in the upper stratosphere. MIPAS C₂H₆ data are restricted to the upper troposphere and lower stratosphere (von Clarmann et al., 2007).

The analysed dataset consisted of 54 days between 8 September 2003 and 25 March 2004 with about 1000 geolocations per day. This period covers the maximum (September/October 2003) and decline (November/December 2003) of the southern hemispheric biomass burning season and the subsequent months (January to March 2004) with nearly no biomass burning activity in the Southern Hemisphere. From September to December 2003, strongly enhanced HCN and C₂H₆ amounts extended from South America over South Atlantic, South Africa, Indian Ocean, Australia to the South Pacific, showing a distinct biomass burning plume. In the subsequent months these HCN and C₂H₆ amounts had strongly decreased, and in March 2004 the HCN plume had nearly disappeared. The tropospheric lifetime of HCN estimated from this decline is 6.3–6.7 months, which is in fairly good agreement with the value of 5.3 months given by Li et al. (2003). Generally there was good agreement of the spatial coverage of enhanced southern hemispheric HCN and C₂H₆. However, especially in September and October 2003 MIPAS measured high C₂H₆ but low HCN amounts in the region between the mid-Pacific and Ecuador/Peru. Except for the upper troposphere above South East Asia in September, enhanced northern hemispheric HCN was only observed in considerably smaller regions above the tropical Atlantic and the Middle East. On the contrary there was an equally pronounced northern hemispheric C₂H₆ signature, extending from the tropics northward to midlatitudes.

The occurrence of plumes with high C₂H₆ and low HCN can be explained by the typical sources of both pollutants: HCN is mainly produced by biomass burning, whereas the sources of C₂H₆ are industrial activities like fossil fuel production or transmission as well as biomass burning. HYSPLIT backward trajectory calculations were used for selected air masses to analyse the origin and possible sources of

pollution. These backward trajectories indicated that the high C₂H₆ amounts measured in September 2003 over the Galapagos region had been injected into the free troposphere over northern South America. Since biomass burning activity in this region was low during September 2003, we conclude that these elevated C₂H₆ amounts were caused by the local fossil fuel production. The high C₂H₆ over the Caribbean Sea and the Gulf of Mexico could also be related to fossil fuel production in northern South America and to a certain extent in Northern Africa and South Asia. As shown by backward trajectory calculations in Funke et al. (2009), the high C₂H₆ amounts in the Asian monsoon anticyclone in September 2003 originated from urban or industrial pollution in Bangladesh and Southeast China. The high HCN found in the uppermost part of the anticyclone suggests South-Asian biomass burning as additional source. Further, we identified fossil fuel production in Indonesia and Northern South America as possible sources for the elevated C₂H₆ amounts measured at the West Coast of North America in December 2003. Thus generally all regions of high C₂H₆ but low HCN could be associated to industrial or urban pollution. This leads to definition of a chemical fingerprint of the observed air masses: From September to December 2003 the C₂H₆/HCN ratios were typically between 1 and 1.5 in the southern biomass burning plume and larger than 1.5 (up to 3) in air masses polluted by industrial activities. However in March 2003 ratios of 2 were also obtained in some regions of the former biomass burning plume.

The southern hemispheric MIPAS HCN distribution shows good spatial agreement with the CO distribution measured by the MOPITT experiment during late September 2003, which is also attributed to biomass burning. Unfortunately there are no other spaceborne measurements of tropospheric HCN and C₂H₆ available for the time period investigated here. However, there is qualitatively good accordance of the biomass burning plume observed by MIPAS with the HCN and C₂H₆ distributions measured between September and November 2005 by the Fourier Transform Spectrometer (FTS) on the ACE/SCISAT-1 satellite. The background and elevated HCN amounts measured by MIPAS are, at least, in good agreement with airborne in-situ measurements performed in earlier years. There is also good consistency with upper tropospheric HCN amounts measured by ground-based FTIR spectroscopy in Australia.

Acknowledgements. The authors like to thank the European Space Agency for giving access to MIPAS level-1 data. The retrievals were performed on the HP XC4000 of the Scientific Supercomputing Center (SSC) Karlsruhe under project grant MIPAS. Meteorological analysis data have been provided by ECMWF. The IMK team has partially been supported by funds of the IMACCO project. The IAA team was supported by the Spanish MICINN under contract AYA2008-03498 and EC FEDER funds. NCEP Reanalysis data were provided by the NOAA/OAR/ESRL PSD, Boulder, Colorado, USA, from their Web site at <http://www.cdc.noaa.gov>. The HYSPLIT transport

and dispersion model was supplied by the NOAA Air Resources Laboratory (ARL).

Edited by: T. Karl

References

- Aikin, A. C., Herman, J. R., Maier, E. J., and McQuillan, C. J.: Atmospheric Chemistry of Ethane and Ethylene, *J. Geophys. Res.*, 87(C4), 3105–3118, 1982.
- Bertschi, I. T., Yokelson, R. J., Ward, D. E., Christian, T. J., and Hao, W. M.: Trace gas emissions from the production and use of domestic biofuels in Zambia measured by open-path Fourier transform infrared spectroscopy, *J. Geophys. Res.*, 108, D8469, doi:10.1029/2002JD002158, 2003.
- Cicerone, R. J. and Zellner, R.: The Atmospheric Chemistry of Hydrogen Cyanide (HCN), *J. Geophys. Res.*, 88(C15), 10689–10696, 1983.
- Coffey, M. T., Mankin, W. G., and Cicerone, R. J.: Spectroscopic detection of stratospheric hydrogen cyanide, *Science*, 214, 333–335, 1981.
- Coheur, P.-F., Herbin, H., Clerbaux, C., Hurtmans, D., Wespes, C., Carleer, M., Turquety, S., Rinsland, C. P., Remedios, J., Hauglustaine, D., Boone, C. D., and Bernath, P. F.: ACE-FTS observation of a young biomass burning plume: first reported measurements of C₂H₄, C₃H₆O, H₂CO and PAN by infrared occultation from space, *Atmos. Chem. Phys.*, 7, 5437–5446, 2007, <http://www.atmos-chem-phys.net/7/5437/2007/>.
- Crouse, J. D., DeCarlo, P. F., Blake, D. R., Emmons, L. K., Campos, T. L., Apel, E. C., Clarke, A. D., Weinheimer, A. J., McCabe, D. C., Yokelson, R. J., Jimenez, J. L., and Wennberg, P. O.: Biomass burning and urban air pollution over the Central Mexican Plateau, *Atmos. Chem. Phys.*, 9, 4929–4944, 2009, <http://www.atmos-chem-phys.net/9/4929/2009/>.
- Draxler, R. R.: The accuracy of trajectories during ANATEX calculated using dynamic model analyses versus Rawinsonde observations, *J. Appl. Meteorol.*, 30, 1446–1467, 1991.
- Draxler, R. R. and Hess, G. D.: An overview of the HYSPLIT.4 modelling system for trajectories, dispersion, and deposition, *Aust. Meteorol. Mag.*, 47, 295–308, 1998.
- Edwards, D. P., Emmons, L. K., Gille, J. C., Chu, A., Attié, J.-L., Giglio, L., Wood, S. W., Haywood, J., Deeter, M. N., Massie, S. T., Ziskin, D. C., and Drummond, J. R.: Satellite-observed pollution from Southern Hemisphere biomass burning, *J. Geophys. Res.*, 111, D14312, doi:10.1029/2005JD006655, 2006.
- European Space Agency: Envisat, MIPAS An instrument for atmospheric chemistry and climate research, ESA Publications Division, ESTEC, P.O. Box 299, 2200 AG Noordwijk, The Netherlands, SP-1229, 2000.
- Fischer, H., Birk, M., Blom, C., Carli, B., Carlotti, M., von Clarmann, T., Delbouille, L., Dudhia, A., Ehnhalt, D., Endemann, M., Flaud, J. M., Gessner, R., Kleinert, A., Koopman, R., Langen, J., López-Puertas, M., Mosner, P., Nett, H., Oelhaf, H., Perron, G., Remedios, J., Ridolfi, M., Stiller, G., and Zander, R.: MIPAS: an instrument for atmospheric and climate research, *Atmos. Chem. Phys.*, 8, 2151–2188, 2008, <http://www.atmos-chem-phys.net/8/2151/2008/>.
- Funke, B., López-Puertas, M., García-Comas, M., Stiller, G. P., von Clarmann, T., Höpfner, M., Glatthor, N., Grabowski, U., Kellmann, S., and Linden, A.: Carbon monoxide distributions from the upper troposphere to the mesosphere inferred from 4.7 μm non-local thermal equilibrium emissions measured by MIPAS on Envisat, *Atmos. Chem. Phys.*, 9, 2387–2411, 2009, <http://www.atmos-chem-phys.net/9/2387/2009/>.
- Giglio, L., Kendall, J. D., and Tucker, C. J.: Remote sensing of fires with the TRMM VIRS, *Int. J. Remote Sens.*, 21, 203–207, 2000.
- Glatthor, N., von Clarmann, T., Fischer, H., Funke, B., Grabowski, U., Höpfner, M., Kellmann, S., Kiefer, M., Linden, A., Milz, M., Steck, T., Stiller, G. P., Mengistu Tsidu, G., and Wang, D.-Y.: Spaceborne ClO observations by the Michelson Interferometer for Passive Atmospheric Sounding (MIPAS) before and during the Antarctic major warming in September/October 2002, *J. Geophys. Res.*, 109, D11307, doi:10.1029/2003JD004440, 2004.
- Glatthor, N., von Clarmann, T., Fischer, H., Funke, B., Grabowski, U., Höpfner, M., Kellmann, S., Kiefer, M., Linden, A., Milz, M., Steck, T., and Stiller, G. P.: Global peroxyacetyl nitrate (PAN) retrieval in the upper troposphere from limb emission spectra of the Michelson Interferometer for Passive Atmospheric Sounding (MIPAS), *Atmos. Chem. Phys.*, 7, 2775–2787, 2007, <http://www.atmos-chem-phys.net/7/2775/2007/>.
- Hough, A. M.: Development of a Two-Dimensional Global Tropospheric Model: Model Chemistry, *J. Geophys. Res.*, 96(D4), 7325–7362, 1991.
- Kalnay, E., Kanamitsu, M., Kistler, R., Collins, W., Deaven, D., Gandin, L., Iredell, M., Saha, S., White, G., Woollen, J., Zhu, Y., Leetmaa, A., and Reynolds, R.: The NCEP/NCAR 40-year reanalysis project, *B. Am. Meteor. Soc.*, 77, 437–470, 1996.
- Kiefer, M., von Clarmann, T., and Grabowski, U.: State parameter Data Base for MIPAS Data Analysis, *Adv. Space Res.*, 30(11), 2387–2392, 2002.
- Kleinert, A., Aubertin, G., Perron, G., Birk, M., Wagner, G., Hase, F., Nett, H., and Poulin, R.: MIPAS Level 1B algorithms overview: operational processing and characterization, *Atmos. Chem. Phys.*, 7, 1395–1406, 2007, <http://www.atmos-chem-phys.net/7/1395/2007/>.
- Li, Q., Jacob, D. J., Yantosca, R. M., Heald, C. L., Singh, H. B., Koike, M., Zhao, Y., Sachse, G. W., and Streets, D. G.: A global three-dimensional model analysis of the atmospheric budgets of HCN and CH₃CN: Constraints from aircraft and ground measurements, *J. Geophys. Res.*, 108(D21), 8827, doi:10.1029/2002JD003075, 2003.
- Lobert, J. M., Scharffe, D. H., Hao, W. M., and Crutzen, P.: Importance of biomass burning in the atmospheric budgets of nitrogen-containing gases, *Nature*, 346, 552–554, 1990.
- Lupu, A., Kaminski, J. W., Neary, L., McConnell, J. C., Toyota, K., Rinsland, C. P., Bernath, P. F., Walker, K. A., Boone, C. D., Nagahama, Y., and Suzuki, K.: Hydrogen cyanide in the upper troposphere: GEM-AQ simulation and comparison with ACE-FTS observations, *Atmos. Chem. Phys.*, 9, 4301–4313, 2009, <http://www.atmos-chem-phys.net/9/4301/2009/>.
- Mahieu, E., Rinsland, C. P., Zander, R., Demoulin, P., Delbouille, L., and Roland, G.: Vertical column abundances of HCN deduced from ground-based infrared solar spectra: Long-term trend and variability, *J. Atmos. Chem.*, 20, 299–310, 1995.
- Mahieu, E., Zander, R., Delbouille, L., Demoulin, P., Roland, G., and Servais, C.: Observed trends in total vertical column abundances of atmospheric gases from IR solar spectra recorded at the Jungfraujoch, *J. Atmos. Chem.*, 28, 227–243, 1997.

- Park, M., Randel, W. J., Emmons, L. K., Bernath, P. F., Walker, K. A., and Boone, C. D.: Chemical isolation in the Asian monsoon anticyclone observed in Atmospheric Chemistry Experiment (ACE-FTS) data, *Atmos. Chem. Phys.*, 8, 757–764, 2008, <http://www.atmos-chem-phys.net/8/757/2008/>.
- Pumphrey, H. C., Jimenez, C. J., and Waters, J. W.: Measurement of HCN in the middle atmosphere by EOS MLS, *Geophys. Res. Lett.*, 33, L08804, doi:10.1029/2005GL025656, 2006.
- Remedios, J. J., Leigh, R. J., Waterfall, A. M., Moore, D. P., Sembhi, H., Parkes, I., Greenhough, J., Chipperfield, M.P., and Hauglustaine, D.: MIPAS reference atmospheres and comparisons to V4.61/V4.62 MIPAS level 2 geophysical data sets, *Atmos. Chem. Phys. Discuss.*, 7, 9973–10017, 2007, <http://www.atmos-chem-phys-discuss.net/7/9973/2007/>.
- Rinsland, C. P., Smith, M. A. H., Rinsland, P. L., Goldman, A., Brault, J. W., and Stokes, G. M.: Ground-based spectroscopic measurements of atmospheric hydrogen cyanide, *J. Geophys. Res.*, 87, 11119–11125, 1982.
- Rinsland, C. P., Gunson, M. R., Wang, P.-H., Arduini, R. F., Baum, B. A., Minnis, P., Goldman, A., Abrams, M. C., Zander, R., Mahieu, E., Salawitch, R. J., Michelsen, H. A., Irion, F. W., and Newchurch, M. J.: ATMOS/ATLAS 3 Infrared Measurements of Trace Gases in the November 1994 Tropical and Subtropical Upper Troposphere, *J. Quant. Spectrosc. Ra.*, 60(5), 891–901, 1998.
- Rinsland, C. P., Goldman, A., Murcray, F. J., et al.: Infrared solar spectroscopic measurements of free tropospheric CO, C₂H₆, and HCN above Mauna Loa, Hawaii: Seasonal variations and evidence for enhanced emissions from the southeast Asian tropical fires of 1997–1998, *J. Geophys. Res.*, 104, 18667–18680, 1999.
- Rinsland, C. P., Mahieu, E., Zander, R., Demoulin, P., Forrer, J., and Buchmann, B.: Free tropospheric CO, C₂H₆, and HCN above central Europe: Recent measurements from the Jungfraujoch station including the detection of elevated columns during 1998, *J. Geophys. Res.*, 105(D19), 24235–24249, 2000.
- Rinsland, C. P., Goldman, A., Zander, R., and Mahieu, E.: Enhanced tropospheric HCN columns above Kitt Peak during the 1982–1983 and 1997–1998 El Niño warm phases, *J. Quant. Spectrosc. Ra.*, 69(1), 3–8, 2001.
- Rinsland, C. P., Jones, N. B., Connor, B. J., Wood, S. W., Goldman, A., Stephen, T. M., Murcray, F. J., Chiou, L. S., Zander, R., and Mahieu, E.: Multiyear infrared solar spectroscopic measurements of HCN, CO, C₂H₆, and C₂H₂ tropospheric columns above Lauder, New Zealand (45° S latitude), *J. Geophys. Res.*, 107(D14), 4185, doi:10.1029/2001JD001150, 2002.
- Rinsland, C. P., Dufour, G., Boone, C. D., and Bernath, P. F.: Atmospheric Chemistry Experiment (ACE) measurements of elevated Southern Hemisphere upper tropospheric CO, C₂H₆, HCN, and C₂H₂ mixing ratios from biomass burning emissions and long range transport, *Geophys. Res. Lett.*, 32, L20803, doi:10.1029/2005GL024214, 2005.
- Rothman, L. S., Jacquemart, D., Barbe, A., et al.: The HITRAN 2004 molecular spectroscopic database, *J. Quant. Spectrosc. Ra.*, 96, 139–204, doi:10.1016/j.jqsrt.2004.10.008, 2005.
- Rudolph, J. and Ehhalt, D. H.: Measurements of C₂-C₅ Hydrocarbons Over the North Atlantic, *J. Geophys. Res.*, 86(C12), 11959–11964, 1981.
- Rudolph, J.: The tropospheric distribution and budget of ethane, *J. Geophys. Res.*, 100(D6), 11369–11381, 1995.
- Singh, H., Chen, Y., Staudt, A., Jacob, D., Blake, D., Heikes, B., and Snow, J.: Evidence from the Pacific troposphere for large global sources of oxygenated organic compounds, *Nature*, 410, 1078, 2001.
- Singh, H. B., Salas, L., Herlth, D., et al.: In situ measurements of HCN and CH₃CN over the Pacific Ocean: Sources, sinks and budgets, *J. Geophys. Res.*, 108(D20), 8795, doi:10.1029/2002JD003006, 2003.
- Steck, T.: Methods for determining regularization for atmospheric retrieval problems, *Appl. Optics*, 41(9), 1788–1797, 2002.
- Stiller, G. P.: The Karlsruhe Optimized and Precise Radiative transfer Algorithm (KOPRA), Institut für Meteorologie und Klimaforschung, Forschungszentrum Karlsruhe GmbH, 2000.
- von Clarmann, T., Fischer, H., Funke, B., Glatthor, N., Grabowski, U., Höpfner, M., Kellmann, S., Kiefer, M., Linden, A., Mengistu Tsidu, G., Milz, M., Steck, T., Stiller, G. P., Wang, D.-Y., Gil-López, S., and López-Puertas, M.: Retrieval of temperature and tangent altitude pointing from limb emission spectra recorded from space by the michelson interferometer for passive atmospheric sounding (MIPAS), *J. Geophys. Res.*, 108(D23), 4736, doi:10.1029/2003JD003602, 2003.
- von Clarmann, T., Glatthor, N., Koukouli, M. E., Stiller, G. P., Funke, B., Grabowski, U., Höpfner, M., Kellmann, S., Linden, A., Milz, M., Steck, T., and Fischer, H.: MIPAS measurements of upper tropospheric C₂H₆ and O₃ during the southern hemispheric biomass burning season in 2003, *Atmos. Chem. Phys.*, 7, 5861–5872, 2007, <http://www.atmos-chem-phys.net/7/5861/2007/>.
- Xiao, Y., Logan, J. A., Jacob, D. J., Hudman, R. C., Yantosca, R., and Blake, D. R.: Global budget of ethane and regional constraints on US sources, *J. Geophys. Res.*, 113, D21306, doi:10.1029/2007JD009415, 2008.
- Yokelson, R. J., Urbanski, S. P., Atlas, E. L., Toohey, D. W., Alvarado, E. C., Crouse, J. D., Wennberg, P. O., Fisher, M. E., Wold, C. E., Campos, T. L., Adachi, K., Buseck, P. R., and Hao, W. M.: Emissions from forest fires near Mexico City, *Atmos. Chem. Phys.*, 7, 5569–5584, 2007, <http://www.atmos-chem-phys.net/7/5569/2007/>.